This paper is published as part of a PCCP Themed Issue on:
Physical Chemistry of Aerosols

Guest Editors: Ruth Signorell and Allan Bertram (University of British Columbia)

Editorial

Perspective

Papers

Laboratory chamber studies on the formation of organosulfates from reactive uptake of monoterpene oxides
Yoshiteru Iinuma, Olaf Böge, Ariane Kahnt and Hartmut Herrmann, *Phys. Chem. Chem. Phys.*, 2009, **DOI:** 10.1039/b904025k

Measurement of fragmentation and functionalization pathways in the heterogeneous oxidation of oxidized organic aerosol
Jesse H. Kroll, Jared D. Smith, Dung L. Che, Sean H. Kessler, Douglas R. Worsnop and Kevin R. Wilson, *Phys. Chem. Chem. Phys.*, 2009, **DOI:** 10.1039/b905289e

Using optical landscapes to control, direct and isolate aerosol particles
Jon B. Wills, Jason R. Butler, John Palmer and Jonathan P. Reid, *Phys. Chem. Chem. Phys.*, 2009, **DOI:** 10.1039/b908270k

Reactivity of oleic acid in organic particles: changes in oxidant uptake and reaction stoichiometry with particle oxidation
Amy M. Sage, Emily A. Weitkamp, Allen L. Robinson and Neil M. Donahue, *Phys. Chem. Chem. Phys.*, 2009, **DOI:** 10.1039/b904285g

Surface tension of mixed inorganic and dicarboxylic acid aqueous solutions at 298.15 K and their importance for cloud activation predictions
Alastair Murray Booth, David Owen Topping, Gordon McFiggans and Carl John Percival, *Phys. Chem. Chem. Phys.*, 2009, **DOI:** 10.1039/b906849j

Kinetics of the heterogeneous conversion of 1,4-hydroxycarbonyls to cyclic hemiacetals and dihydrofurans on organic aerosol particles
Yong Bin Lim and Paul J. Ziemann, *Phys. Chem. Chem. Phys.*, 2009, **DOI:** 10.1039/b904333k

Time-resolved molecular characterization of limonene/ozone aerosol using high-resolution electrospray ionization mass spectrometry
Adam P. Bateman, Sergey A. Nizkorodov, Julia Laskin and Alexander Laskin, *Phys. Chem. Chem. Phys.*, 2009, **DOI:** 10.1039/b905288g

Cloud condensation nuclei and ice nucleation activity of hydrophobic and hydrophilic soot particles
Kirsten A. Koehler, Paul J. DeMott, Sonia M. Kreidenweis, Olga B. Popovicheva, Markus D. Petters, Christian M. Carrico, Elena D. Kireeva, Tatiana D. Khokhlova and Natalia K. Shonija, *Phys. Chem. Chem. Phys.*, 2009, **DOI:** 10.1039/b905334b

Effective broadband refractive index retrieval by a white light optical particle counter
J. Michel Flores, Miri Trainic, Stephan Borrmann and Yinon Rudich, *Phys. Chem. Chem. Phys.*, 2009, **DOI:** 10.1039/b905292e

Influence of gas-to-particle partitioning on the hygroscopic and droplet activation behaviour of α-pinene secondary organic aerosol
Zsófia Jurányi, Martin Gysel, Jonathan Duplissy, Ernest Weingartner, Torsten Tritscher, Josef Dommen, Silvia Henning, Markus Ziese, Alexej Kiselev, Frank Stratmann, Ingrid George and Urs Baltensperger, *Phys. Chem. Chem. Phys.*, 2009, **DOI:** 10.1039/b904162a

Reactive uptake studies of NO_3 and N_2O_5 on alkenoic acid, alkanoate, and polyalcohol substrates to probe nighttime aerosol chemistry
Simone Gross, Richard Iannone, Song Xiao and Allan K. Bertram, *Phys. Chem. Chem. Phys.*, 2009, **DOI:** 10.1039/b904741g

Organic nitrate formation in the radical-initiated oxidation of model aerosol particles in the presence of NO_x
Lindsay H. Renbaum and Geoffrey D. Smith, *Phys. Chem. Chem. Phys.*, 2009, **DOI:** 10.1039/b909239k

Dynamics and mass accommodation of HCl molecules on sulfuric acid–water surfaces
P. Behr, U. Scharfenort, K. Ataya and R. Zellner, *Phys. Chem. Chem. Phys.*, 2009, **DOI:** 10.1039/b904629a

Structural stability of electrosprayed proteins: temperature and hydration effects
Erik G. Marklund, Daniel S. D. Larsson, David van der Spoel, Alexandra Patriksson and Carl Caleman, *Phys. Chem. Chem. Phys.*, 2009, **DOI:** 10.1039/b903846a

Tandem ion mobility-mass spectrometry (IMS-MS) study of ion evaporation from ionic liquid-acetonitrile nanodrops
Christopher J. Hogan Jr and Juan Fernández de la Mora, *Phys. Chem. Chem. Phys.*, 2009, **DOI:** 10.1039/b904022f

Homogeneous ice freezing temperatures and ice nucleation rates of aqueous ammonium sulfate and aqueous levoglucosan particles for relevant atmospheric conditions
Daniel Alexander Knopf and Miguel David Lopez, *Phys. Chem. Chem. Phys.*, 2009, **DOI:** 10.1039/b903750k

A study of oleic acid and 2,4-DHB acid aerosols using an IR-VUV-ITMS: insights into the strengths and weaknesses of the technique

Sarah J. Hanna,[a] Pedro Campuzano-Jost,[a] Emily A. Simpson,[a] Itamar Burak,[b] Michael W. Blades,[a] John W. Hepburn[a] and Allan K. Bertram*[a]

Received 9th March 2009, Accepted 3rd June 2009
First published as an Advance Article on the web 30th June 2009
DOI: 10.1039/b904748d

An investigation of oleic acid and 2,4-dihydroxybenzoic (DHB) acid aerosols was carried out using an aerosol mass spectrometer with pulsed lasers for vaporization and ionization and an ion trap for mass analysis. The extent of ion fragmentation was studied as a function of both vaporization energy and ionization wavelength. Low CO_2 laser energies in the vaporization stage and near-threshold single photon ionization resulted in the least fragmented mass spectra. For DHB, only the molecular ion was observed, but for oleic acid fragmentation could not be eliminated. Tandem MS of the main fragment peak from oleic acid was carried out and provided a tool for compound identification. Photoionization efficiency curves were also collected for both DHB and oleic acid and the appearance energies of both parent and fragment ions were measured. Evidence for fragmentation occurring post-ionization is given by the similar appearance energies for both the parent and fragment ions. The results from this study were compared with those from similar experiments undertaken with time-of-flight (TOF) mass analyzers. The degree of fragmentation in the ion trap was considerably higher than that seen with TOF systems, particularly for oleic acid. This was attributed to the long storage interval in the ion trap which allows time for metastable ions to decay. Differences in the degree of fragmentation between the ion trap and TOF studies also provided further evidence for fragmentation occurring post-ionization. For 2,4-dihydroxybenzoic acid, the long delay prior to mass analysis also allowed time for reactions with background gases, in this case water, to occur.

Introduction

Aerosol particles, which range in size from 2 nm to tens of microns, are ubiquitous in the earth's atmosphere.[1] These particles have a highly varied chemical composition, but a significant mass fraction (20–90%) of the submicron aerosol component is composed of, or contains, organic molecules.[2] These organic aerosols are thought to play an important role in climate, human health, and the chemistry of the atmosphere.[3–5] However, their composition can be extremely complex, presenting a significant challenge to standard analytical techniques.[6,7]

Over the past two decades aerosol mass spectrometry has become an increasingly important tool for analyzing atmospheric aerosols and a wide variety of instruments have been developed for use in both the field and the laboratory.[8–10] The main hurdle in organic aerosol analysis is the fragility of the molecules being studied. Large organic molecules fragment extensively under traditional ionization techniques like electron impact and the resulting mass spectra are often very difficult to interpret, especially if the aerosols contain a mixture of species. In order to circumvent this difficulty, a considerable amount of effort has gone into designing aerosol mass spectrometers which minimize fragmentation of organics. One successful strategy has been separation of the vaporization and ionization stages in combination with soft ionization techniques.[11] Some of the soft ionization methods that have been employed include photoelectron resonance capture ionization (PERCI),[12] chemical ionization (CI),[13,14] metal attachment,[15] resonance enhanced multiphoton ionization (REMPI),[11,16–19] and single photon ionization (SPI).[20–29]

In many aerosol mass spectrometers mass analysis is done with either linear quadrupole or time-of-flight mass analyzers, however ion traps have also been successfully incorporated into several systems.[14,18,30–37] Ion traps have a number of features which make them appealing for aerosol mass spectrometry. They are compact, sensitive, have a large accessible mass range, collect a full mass spectrum for every particle, and have the ability to carry out tandem mass spectrometry. For soft ionization systems in particular, tandem mass spectrometry is a desirable feature since a considerable amount of chemical information is sacrificed when a mass spectrum with only the parent peak is obtained. Tandem mass spectrometry makes it possible to determine not only the structure of the molecular ion, but also the structure of any fragment ions of interest.

In a previous publication we described the design and performance of a VUV-ion trap aerosol mass spectrometer.[38]

[a] *Department of Chemistry, University of British Columbia, Vancouver, Canada BC V6T 1Z1. E-mail: bertram@chem.ubc.ca*
[b] *Department of Chemistry, Tel Aviv University, Tel Aviv, Israel*

This instrument uses a CO_2 laser for vaporization and vacuum UV from pulsed lasers for soft, single photon ionization. Separate vaporization and ionization stages combined with soft ionization are employed to reduce fragmentation; in addition, an ion trap for mass analysis gives the benefit of MS^n capability. In the previous work we showed results for caffeine aerosols vaporized at several CO_2 laser energies and ionized with VUV light at 142 nm (8.75 eV). Caffeine is a robust molecule which has a simple fragmentation pattern with the base peak at the molecular ion mass even under relatively harsh electron impact ionization.[39]

In the caffeine study, fragmentation was negligible at low CO_2 energy, although it was observed for energies above 20 mJ per pulse when using an IR wavelength on resonance with an absorption band in caffeine. The single particle detection limits were very good at the VUV wavelength used (detection limit of $\sim 8 \times 10^5$ molecules or approximately 3.5% of a pure 225 nm particle, assuming that the other compounds present do not increase the background signal level).

In the current work we expand on this previous study by looking at two different aerosol types using several VUV photon energies for ionization. Aerosols of 2,4-dihydroxybenzoic acid (DHB) and oleic acid were chosen because they have very different chemical structures and because both have been studied using single particle time-of-flight (TOF) aerosol mass spectrometers, allowing us to draw comparisons between these instruments and the ion trap device, and to highlight some of the strengths and weaknesses of the VUV-ion trap technique.

Like caffeine, DHB is an aromatic hydrocarbon which forms solid aerosol particles. However, it is slightly less robust than caffeine and with electron impact ionization the base peak corresponds to a water-loss fragment.[39] Oleic acid is a monounsaturated fatty acid with a long carbon chain. It forms liquid aerosol particles and fragments extensively with electron impact ionization.[39,40]

In the following we look at the mass spectra for these two molecules as a function of both the vaporization energy and the ionization wavelength. When using low vaporization energies and near-threshold ionization, only the molecular ion is observed for DHB, whereas for oleic acid extensive fragmentation occurs even under the gentlest conditions and only a small amount of the molecular ion is seen. Significant differences between the results from the ion trap experiments and those performed using time-of-flight mass spectrometers were observed and are discussed in detail. In some cases SPI was replaced with REMPI to provide a better match with the reference studies and to highlight the differences in the results obtained with single photon ionization. The results of this study demonstrate that the ion trap has significant advantages over TOF systems when using low CO_2 laser powers to analyze more stable compounds like caffeine and DHB. Even for less stable compounds like oleic acid, the ion trap will give information complementary to that obtained with TOF instruments.

The analytical capabilities of the VUV-ion trap instrument are also further explored in this work. Detection limits are calculated for both DHB and oleic acid aerosols at two VUV wavelengths (142 nm and 124 nm), photoionization efficiency (PIE) curves are shown with both molecular ion and fragment appearance energies measured, and the accuracy in determining appearance energies is discussed.

Experimental

2.1 Particle generation

Aerosols for these experiments were made from solutions of either pure 2,4-dihydroxybenzoic acid (Fluka, $\geq 98\%$) or pure oleic acid (Sigma-Aldrich, $\geq 99\%$). The DHB solutions were made with filtered Millipore (18 MΩ) water and the oleic acid solutions were made in 2-propanol (Aldrich, 99.9%). In both cases the chemicals were used without further purification. Oleic acid aerosols one micron in diameter were generated from dilute ($\sim 1 \times 10^{-5}$ g ml^{-1}) solutions using a TSI vibrating orifice aerosol generator (VOAG, TSI Inc., Model 3450). DHB aerosols 600 nm in diameter were generated from more concentrated solutions ($\sim 1 \times 10^{-3}$ g ml^{-1}) using a TSI constant output atomizer (TSI Inc., Model 3076). Since the constant output atomizer generates aerosols with a very broad size distribution, these particles were size selected with a TSI DMA (TSI Inc., Model 3081) prior to analysis. Size selection was done to reduce the number of small particles (<150 nm) impacting on the ion trap electrodes and vacuum manifold, which could potentially lead to contamination in the mass spectrometer over several months of experiments. The vibrating orifice aerosol generator produces a much narrower size distribution and particles generated using this method were analyzed directly.

All aerosols were passed through an ^{85}Kr charge neutralizer (TSI Inc., Model 3054) before entering the vacuum region of the aerosol mass spectrometer. This acted as a drying tube and prevented additional drying and size changes in the aerosol lens. Those particles made with the constant output atomizer were also passed through a 24″ Nafion diffusion dryer (Permapure Inc) prior to entering the DMA.

2.2 Aerosol mass spectrometer

The aerosol mass spectrometer used in these studies is shown schematically in Fig. 1. It has been described in detail elsewhere[40] and only a brief overview will be given here.

The main components of the system are an aerosol inlet, a sizing region, and a particle analysis region where aerosols are vaporized by a pulsed CO_2 laser, the free molecules photoionized by pulsed VUV or UV light, and the ions mass analyzed by an ion trap mass spectrometer.

Particles are drawn into the instrument through an aerodynamic lens which consists of a series of apertures modeled after Liu *et al.*[41,42] The aerodynamic lens focuses the particles into a tight stream which then passes through a skimmer and enters the sizing region. In the sizing region the scattered light from two 532 nm *cw* Nd:YAG lasers (Excelsior 532 Single Mode, Spectra Physics) is detected and used to determine particle velocities. These velocities are recorded by an FPGA board (PCI-7831R, National Instruments) and used to generate the laser triggers. The FPGA board also records information such as the laser powers and the scattering signal intensity for the analyzed particles.

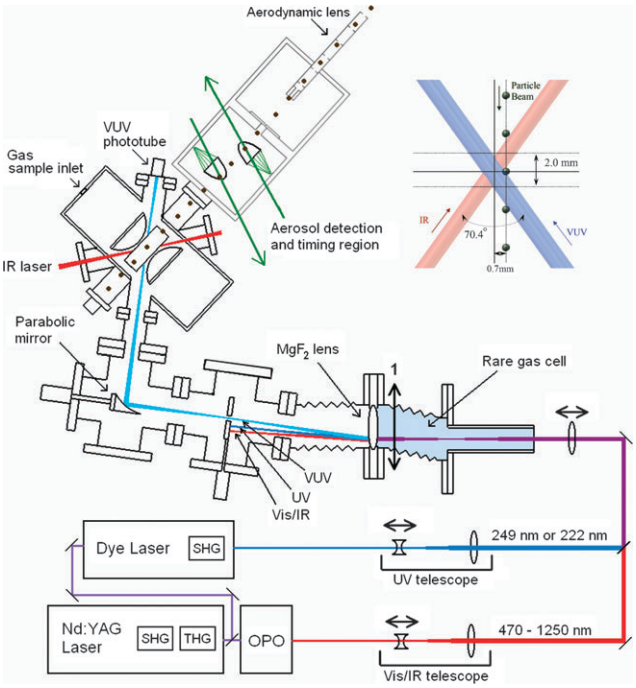

Fig. 1 Instrument schematic.

After exiting the sizing region, the particles enter the ion trap mass spectrometer through a 2 mm hole in the ring electrode where they are vaporized, ionized, and mass analyzed.

In these studies between 5 and 40 mJ of IR light from a pulsed TEA-CO_2 laser (MTL-3G, Edinburgh Instruments) was used to vaporize the particles. The CO_2 laser is tunable over 60 lines between 1087 cm^{-1} (9.2 μm) and 926 cm^{-1} (10.8 μm), and for this work was used at 944 cm^{-1} (10.6 μm).

In these experiments the particles were optically thin with respect to the IR energy and were therefore expected to be uniformly heated by the CO_2 laser pulse. A particle can be defined as optically thin if the product of the radius, r, the absorption cross-section, σ, and the concentration, C, is $\ll 1$.[29] The IR absorption cross-sections of bulk (non-particle) DHB and oleic acid were measured using a Bruker Equinox 55 FTIR. At 944 cm^{-1} the absorption cross-sections were measured to be $(1.05 \pm 0.07) \times 10^{-19}$ and $(2.3 \pm 1.0) \times 10^{-20}$ cm^2 per molecule for oleic acid and DHB, respectively. Based on these numbers $r\sigma C \ll 1$ for these experimental conditions. In addition the particles were small in comparison with the wavelength of the CO_2 laser making it unlikely that internal focusing of the IR light would give rise to a temperature gradient in the particle.[29]

Once the particles were vaporized, molecules in the expanding vapor plume were ionized with either vacuum UV light from a custom built tunable VUV source or by REMPI using UV light from a pulsed dye laser (Sirah PrecisionScan SL). The delay between vaporization and ionization was varied from 0.5 to 30 μs.

The VUV light source has been described in detail elsewhere[38] and will only briefly be reviewed here. In this system VUV is produced by resonance enhanced four wave difference mixing in xenon gas. The source is continuously tunable from 10.2 eV (122 nm) to 7.4 eV (168 nm) and produces between 10^{10} and 10^{13} photons per pulse depending on wavelength. The generated VUV is separated from the pump wavelengths by a custom monochromator and focused to a slightly vertically elongated spot with an area of ~ 1 mm^2. For the REMPI experiments, UV light with a pulse energy of ~ 300 μJ was focused to a spot size of roughly 1.5 mm^2 with the same elongated shape as in the VUV case.

The vaporization and ionization pulses were admitted through the two diagonal paths between the ring and endcap electrodes (Fig. 1). The energy for both was measured after exiting the ion trap. For the CO_2 laser a power meter with a thermal detector (Ophir Model 3A-SH) was used to measure the average IR power. For the VUV a fast phototube (Hamamatsu, R1328U-54) was used to measure the single-shot energy. In the case of the UV light a fraction of the pulse energy was detected with a fast photodiode, the response of which was calibrated using a power meter with a thermal detector (Ophir Model 12A-P).

In the current setup the paths of the vaporization and ionization lasers and the path of the particle beam do not intersect in the center of the trap. Instead the particles first pass through the IR and then the VUV or UV beam as they traverse the ion trap (inset of Fig. 1). The distance that the aerosols travel between the two intersection points is on the order of 2 mm. This was measured by increasing the power of both the IR and UV laser so that ions were generated by each one independently. Varying the timing of the firing in these single laser experiments made it possible to determine the location of the two beams relative to the particles. As a result of this distance, there is no ion signal if the ionization pulse is fired immediately after the CO_2 laser. However, if the delay between the two laser pulses is varied, a profile of the expanding plume from the vaporized aerosol can be obtained (Fig. 2). The shape of this profile is primarily dependent on the distance between the two laser beams and the translational energy of the vaporized molecules which expand outward from the particle, filling, and then passing beyond the ionization volume. The translational energy of the expanding plume is

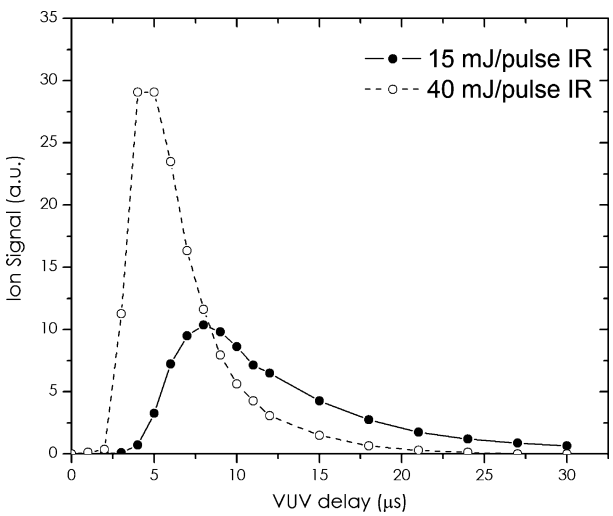

Fig. 2 The evolution of the total ion signal for oleic acid as a function of the delay between vaporization and ionization at two CO_2 laser energies.

highly dependent on the vaporization energy and, as a result, the time at which the ion signal reaches its peak can vary significantly with the CO_2 laser power (Fig. 2). In addition, the internal energy of the molecules varies with the delay between the vaporization and ionization pulses.[43] As a result, the fraction of the total ion signal that comes from the parent and fragment ions varies with the ionization delay, with a proportionate increase in molecular ion signal at longer delay times, in agreement with results seen by Nash *et al.*[26] The dynamics of the plume expansion and the information that this conveys about the particle heating will be explored in detail in a future publication. For this study full scans of the ionization delay time were obtained and the results presented are from an average of several hundred shots at the delay which gave the maximum total ion signal, a strategy similar to that of Nash *et al.*[26]

In all cases the ion trap was operated in mass selective instability mode.[44] Prior to ejection the ions were collisionally cooled for 10 ms in approximately 1 mTorr of helium gas. Supplemental ac waveforms can also be applied to the endcap electrodes in order to perform tandem mass spectrometry or to conduct mass scans in resonant ejection mode, which gives extension of the available mass range.[45] In these experiments tandem mass spectrometry was implemented by applying supplemental SWIFT waveforms[45–48] to the endcaps using custom Labview (National Instruments) software. After ion formation, trapping, and cooling, the selected mass was isolated by applying two rounds of notched broadband waveforms for 5 ms and 3 ms with widths of 15 Da and 2 Da, respectively. The isolated ions then underwent collisional induced dissociation with He buffer gas for 20 ms, followed by collisional cooling and mass analysis.

Mass calibration of the ion trap was done using 70 eV electron impact analysis of small amounts of perfluorotributylamine. Mass scans were performed at a scanning speed of 4000 Da s^{-1}, with a mass resolution under these conditions of $\sim$500 m Δm^{-1} at m/z = 264.

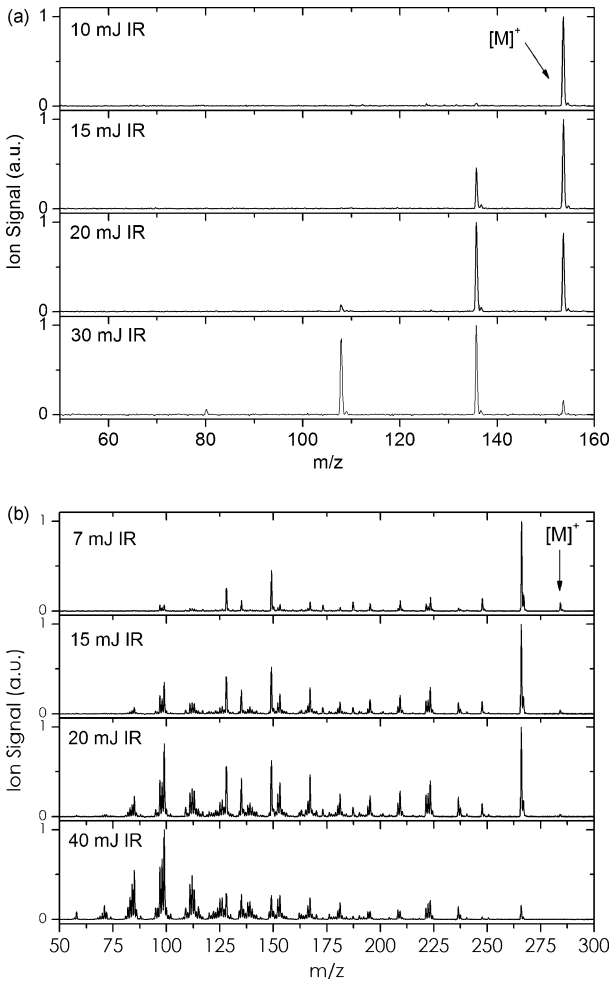

Fig. 3 Mass spectra of (a) DHB and (b) oleic acid as a function of CO_2 laser energy. For DHB the spectra were taken with 10, 15, 20, and 25 mJ per pulse of CO_2 laser energy at 944 cm^{-1} and a VUV wavelength of 142 nm. For oleic acid the spectra were taken with 5, 15, 20, and 40 mJ per pulse of CO_2 laser energy at 944 cm^{-1} and a VUV wavelength of 142 nm.

Results and discussion

3.1 Mass spectra as a function of vaporization energy (with near-threshold ionization)

Fig. 3 shows mass spectra from DHB and oleic acid aerosols vaporized with several different CO_2 laser energies and ionized using the same, near-threshold, VUV photon energy of 8.75 eV (142 nm). These mass spectra are presented in the same manner as the previously reported results for caffeine aerosols which were also vaporized at several CO_2 pulse energies and ionized at 8.75 eV.[38]

For any given aerosol type it can be seen that the extent of fragmentation is heavily dependent on the CO_2 laser energy used for vaporization, a result consistent with observations by other groups that the degree of fragmentation is a strong function of particle heating, regardless of the soft ionization method chosen.[21,22,24,26–28] It can also be seen that the degree of fragmentation is dependent on the type of molecule being studied. For caffeine, almost no fragmentation was seen until quite high vaporization energies were reached ($\sim$20 mJ per pulse), whereas for oleic acid an equivalent energy leaves only 5% of the total signal coming from the molecular ion. DHB is an intermediate case, at low CO_2 laser energy only the molecular ion is observed, but at higher energies it is reduced to a minor component of the mass spectrum.

Preliminary results were also obtained for linolenic acid aerosols. Like oleic acid, linolenic acid is a long chain fatty acid with 18 carbon atoms, however, it contains three double bonds in contrast to oleic acid's one. For linolenic acid aerosols vaporized with low energy CO_2 pulses (5 mJ per pulse), only $\sim$2% of the total ion signal is from the molecular ion. To some extent the differences in fragmentation of the species studied here may be a result of the differences in IR absorption cross-sections of the molecules. For example, at 944 cm^{-1} linolenic acid has an IR absorption cross-section almost twice that of oleic acid (estimated from literature spectra with absorbance normalized to the C=O band)[49] which could result in the much lower abundance of molecular ion that was observed.

Although it causes increased fragmentation, the benefit of high CO_2 laser energy is that a higher fraction of the aerosol is being vaporized. This results in a higher total ion signal which can give lower detection limits by improving the signal to noise ratio.

Although at low CO_2 laser energy it is unlikely that the entire particle is being vaporized, the combination of low vaporization energy and near-threshold ionization gives the benefit of relatively simple mass spectra. For caffeine and DHB only the molecular ion is observed and in cases like these tandem MS can be used to positively identify organics even in complex mixtures.

Oleic and linolenic acids, on the other hand, have very little molecular ion remaining even at low vaporization energies. Nevertheless, the fragmentation patterns for oleic and linolenic acid at low vaporization energies are biased towards a few large, high m/z fragments. These high m/z fragments could be used as markers and targets for tandem MS (see Section 3.4). We also expect to see reduced fragmentation, and thus increased ease of molecular identification, for systems containing other aromatics and shorter chain *n*-alkanes, *n*-alkenes, ketones, and carboxylic acids. These classes of molecules have been shown to have higher stability with 10.5 eV SPI[50,51] and shorter chain lengths mean that less CO_2 energy will be required to vaporize the particles.

The fragmentation observed in the aerosol mass spectra for oleic acid is more than initially expected based on previous aerosol studies that incorporated an IR laser for vaporization, soft photoionization, and TOF-MS for mass analysis.[26] The differences between the ion trap results and previous TOF-MS results are discussed in detail in Section 3.4.

3.2 Mass spectra as a function of VUV energy

One of the strengths of this approach is that the tunable VUV source allows the photon energy to be set very close to the ionization threshold of a molecule of interest. This near-threshold technique should reduce the amount of fragmentation by depositing very little excess energy in the molecule during ionization. This strategy has been successful in other aerosol experiments using TOF mass spectrometers,[25,26] but it has not been previously demonstrated for a VUV ion trap combination. The mass spectra in Fig. 3 show that the molecular ion signal is seen for both DHB and oleic acid, but they do not demonstrate the effectiveness of near-threshold ionization in reducing the amount of fragmentation.

In Fig. 4 mass spectra from DHB and oleic acid aerosols that were vaporized at two different CO_2 pulse energies and ionized with two different VUV wavelengths are shown. The impact of changing the VUV photon energy at both low and high CO_2 laser energies is discussed below.

3.2.1 Low CO_2 laser energy. At low vaporization energy the benefit of near-threshold ionization can be clearly seen for both DHB and oleic acid. For DHB at low CO_2 energy (10 mJ per pulse) and with near-threshold ionization (8.75 eV, 142 nm) only the molecular ion is seen. In contrast, if the VUV photon energy is raised to 10.0 eV (124 nm), the molecular ion accounts for only 70% of the total ion signal, with the remaining 30% coming from the water-loss peak (at m/z 136).

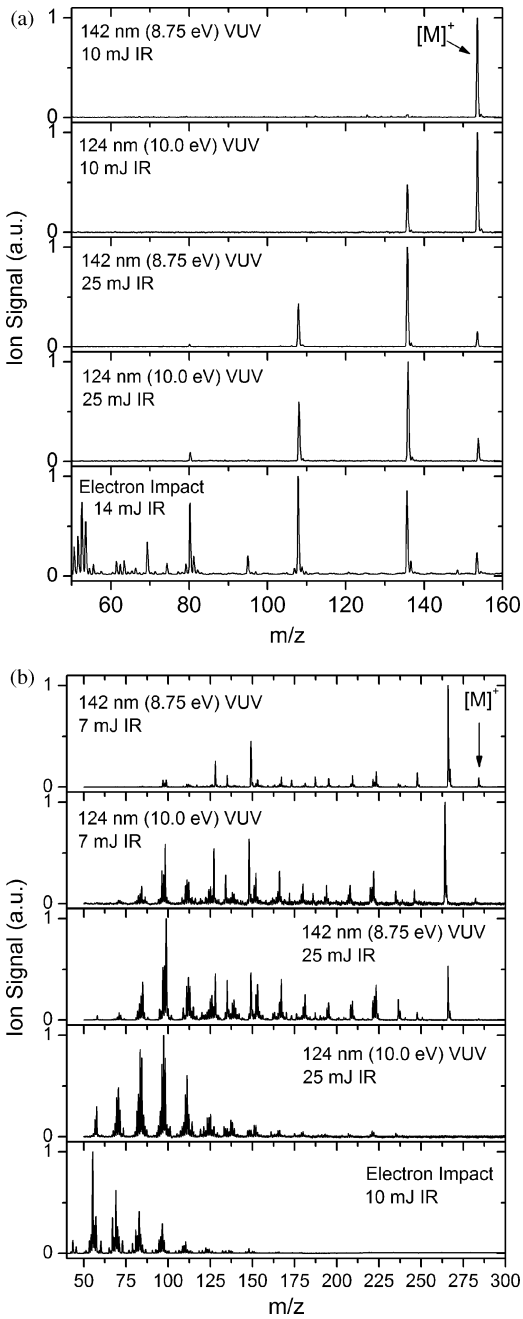

Fig. 4 (a) DHB and (b) oleic acid mass spectra as a function of vaporization energy and ionization wavelength. In all cases the spectra were normalized to the most abundant ion peak and therefore care should be taken when comparing the peak intensities for different experimental conditions.

This higher photon energy is typical of many VUV sources which employ 10.5 eV radiation produced by tripling the third harmonic of an Nd:YAG laser.

For oleic acid vaporized with low CO_2 energy (7 mJ per pulse) there is some fragmentation at both VUV wavelengths, but the near-threshold spectrum is considerably less complicated. At 8.75 eV there are no fragments below m/z 100 and most of the ion signal comes from only a few prominent species. The largest peak is from the water-loss fragment at m/z 264, and some molecular ion is seen at m/z 282. When the VUV energy

is raised to 10.0 eV the molecular ion signal is virtually eliminated and the abundance of fragment peaks is considerably increased.

When compared to electron impact ionization, the benefits of near-threshold ionization are obvious for both DHB and oleic acid. For DHB, electron impact ionization even at low CO_2 energies results in extensive fragmentation, with only 4% of the total ion signal coming from the molecular ion (this is without considering the possibility of very low mass fragments below the mass range used in these experiments). For oleic acid, electron impact ionization with relatively low CO_2 energy results in extensive fragmentation, with no molecular ion signal, and almost no ion signal at all above m/z 100.

3.2.2 High CO_2 laser energy. For oleic acid the benefit of near-threshold ionization even at high CO_2 energy (25 mJ per pulse) is fairly clear. At 8.75 eV there is a prominent peak at m/z 264 and few fragments below m/z 75. At 10.0 eV there is virtually no signal above m/z 175 and considerable signal below m/z 75. For DHB the benefit of near-threshold ionization is less clear at high CO_2 energies. At 25 mJ per pulse the molecular ion accounts for 10% and 12% of the total ion signal at 8.75 and 10.0 eV, respectively. On the other hand, with 10.0 eV ionization the lower mass fragments (108 and 80 m/z) become more prominent.

3.3 Determining ionization energies

Another benefit of a tunable VUV source is the ability to obtain photoionization efficiency curves which can be used to identify compounds by their appearance energies. Fig. 5 shows the photoionization efficiency curves for DHB and oleic acid. These were obtained by continuously scanning the VUV wavelength and recording both the ion signal and the VUV power for each laser shot. Scan speeds were on the order of 0.005 nm s^{-1} (0.0003 eV s^{-1} at 140 nm) and spectra were recorded 3–4 times per second to give a resolution of $\sim$0.002 nm (0.0001 eV). Any fluctuations in the VUV intensity were compensated by normalizing the ion signal to the recorded VUV power. The ability to measure an appearance energy for caffeine was demonstrated in a previous publication.[38] Here we also measure appearance energies for the DHB and oleic acid parent and fragment ions. The measured appearance energies for the molecular ions of DHB and oleic acid are 8.42 ± 0.05 eV and 8.65 ± 0.05 eV, respectively (black traces in Fig. 5). The uncertainty in these measurements arises mainly from the uncertainty in fitting a line to the linear portion of the PIE curve. The ionization energy for oleic acid has been previously measured as 8.68 eV[25] and the appearance energy measured here agrees well with this value.

Although the ability to identify compounds by their appearance energy can be quite useful in determining aerosol constituents,[27] it should be noted that for small particles or low abundance components, signal to noise issues may make collection and interpretation of PIE curves more difficult. In such cases many spectra can be collected and averaged at discreet VUV wavelengths to construct PIE curves, although this will of course be time consuming. In addition, uncertainty in fitting the linear portion of the PIE curves can be reduced by acquiring points over a broader VUV wavelength range.

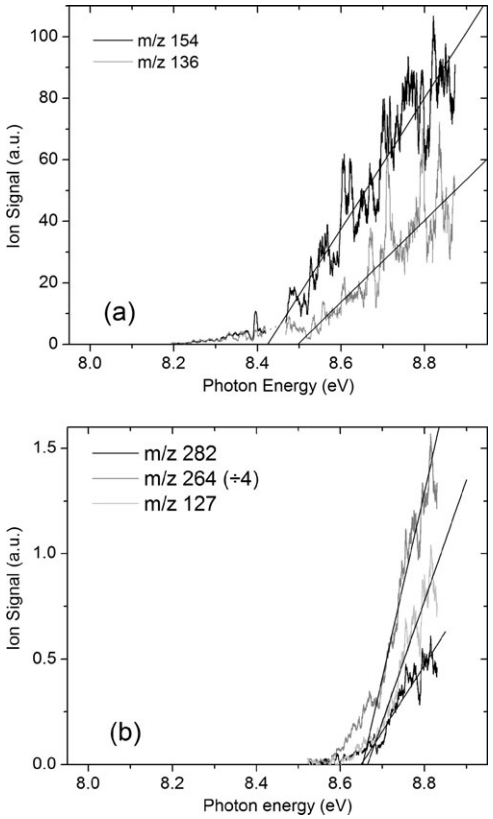

Fig. 5 Photoionization efficiency curves for (a) DHB and (b) oleic acid. The molecular ion peaks are at m/z 154 for DHB and m/z 282 for oleic acid. The break in the DHB curve from 8.42 to 8.48 eV occurs because a strong resonance line in xenon prevents VUV generation in this region.

An interesting feature of the PIE curves is that the individual fragment ions all show roughly the same appearance energies as the molecular ion for both DHB and oleic acid (Fig. 5). For DHB a low vaporization energy was used and only a single fragment at m/z 136 was observed. This fragment had an appearance energy of 8.50 eV, 0.08 eV higher than the molecular ion. It is possible that the appearance energy for this fragment is in fact slightly higher than that of the molecular ion, but since both measurements have an uncertainty of 0.05 eV, we cannot conclusively say that it is different. For oleic acid the parent and fragment ions all appear at the same VUV photon energy. Fig. 5 shows representative traces for high and low mass oleic acid fragments at m/z 264 and m/z 127.

An interesting question that arises for these systems is whether fragmentation occurs before or after ionization.[20,25,26] Two scenarios are possible; in the first scenario the molecule is fragmented during vaporization and the neutral fragments are then ionized by the VUV light. In the second scenario the neutral molecule generated during vaporization, is subsequently ionized by the VUV light, and then decays to give fragments post-ionization. The fact that we observe the same appearance energies for the molecular ion and the fragment ions supports the case of fragmentation occurring post-ionization, a reasonable possibility given the generally lower dissociation energies of ionic species. If a series of neutral fragments were to be

ionized, the appearance energies would almost certainly be different. One would expect this to be especially true in the case of oleic acid where the m/z 282 and m/z 127 ions are likely to have quite different structures, although for DHB the fragment is similar enough in structure to the parent molecule that this interpretation might not apply. In addition to the appearance energies, a comparison of the mass spectra obtained with the VUV-ion trap system and a VUV-TOF system also supports fragmentation occurring post-ionization. This is discussed in detail in Section 3.4.

The most probable scenario regarding fragmentation seems to be that the vaporization step imparts enough internal energy to the molecule to let it dissociate after ionization even with very low VUV photon energies, making the appearance energies of the fragments the same as that of the molecular ion. Such a shift to lower fragment appearance energies with particle heating was observed by Wilson *et al.* in a study of tryptophan aerosols using a heater for vaporization.[52] However, although high internal energy can shift the appearance energy of fragments arising from an ionized molecule, it has only a small effect on the cross-sections of polyatomic neutral molecules and very little change in the molecular ion appearance energy is expected.[53,54] This makes identification of molecules using appearance energies possible even with considerable heating.

3.4 Comparison with results from TOF mass spectrometers

Both DHB and oleic acid have been studied previously in other single particle aerosol mass spectrometers, allowing a comparison of the results from this study with the results from time-of-flight systems.

Nash *et al.* studied 3–4 μm oleic acid particles using a CO_2 laser for vaporization and VUV generated by pulsed lasers for single photon ionization.[26] The mass analysis in their system was done using a TOF mass spectrometer, but the conditions for vaporization and ionization were very similar to those used in this study.

Nash *et al.* reported the ratio of parent to total ion signal as a function of the CO_2 laser energy. We have re-plotted their data in Fig. 6a along with the data from this study. It can be seen that fragmentation is much more extensive in the ion trap experiments than in the work of Nash *et al.* We believe that this disparity occurs because of the type of mass spectrometer used and the resulting difference in the time that the ions are stored prior to mass analysis.

In their study Nash *et al.* noted that if the extraction pulse in their TOF mass spectrometer was delayed by 3 μs, the ratio of the molecular ion to the water-loss fragment decreased from 1.72 to 1.27, an effect they attributed to the decay of a metastable oleic acid molecular ion with a low dissociation rate constant. Using these ratios we can calculate an approximate rate constant for the decay of the metastable oleic acid ion which gives a half-life on the order of several tens of microseconds. In the ion trap, residence times for the ions are on the order of tens of milliseconds. Helium gas is introduced to cool the ions and collisions with helium should thermalize and therefore stabilize the metastable ions. However, at the 1 mTorr pressure used in the trap, the collision rate with helium is on the order of 1 per 120 μs. Even considering the upper limit for cooling, where only a single collision with helium is required to quench the excited oleic acid ion, there is still ample time for the metastable ions to dissociate. The fact that we calculate an approximate half-life on the order of several tens of microseconds from the Nash data means that

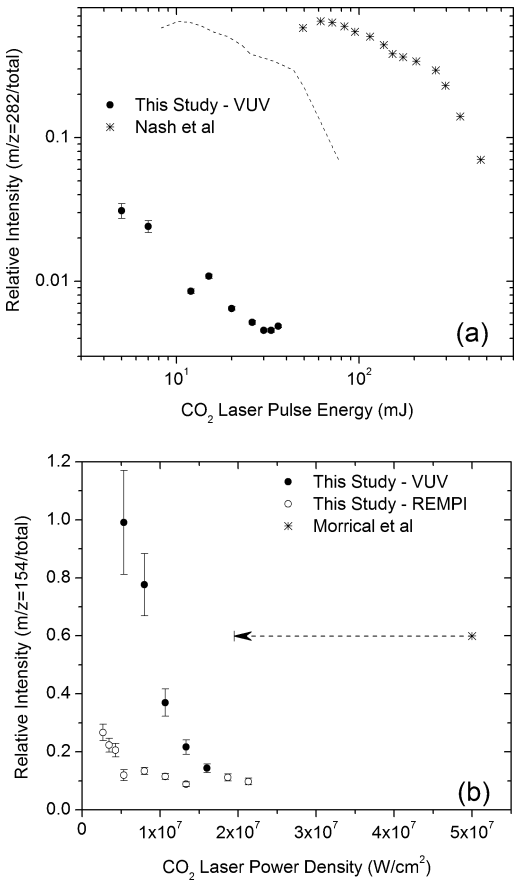

Fig. 6 A comparison of this study with the studies of (a) Nash *et al.*[26] and (b) Morrical *et al.*[11] The ratio of parent to total ion signal is plotted as a function of (a) the vaporization pulse energy or (b) power density depending on the units used in the original work. In this study a TEA pulsed CO_2 laser was used at 944 cm^{-1} (10.6 μm). The laser focus has a Gaussian spatial profile with a FWHM of 0.9 mm and a total pulse duration of ~1 μs with a sharp 150 ns wide spike at the beginning of the pulse accounting for approximately 50% of the total energy. Based on a different study from the same group[66] we assume that for Nash *et al.* the CO_2 laser spot was 0.9 mm and the pulse duration was 140 ns. Given the similarity of the two pulses, the points in (a) are not corrected for any differences in beam profile or pulse duration. The dotted line in (a) shows a lower limit for the values of Nash *et al.* if a correction is made for differences in the dependence of total ion signal on CO_2 laser energy (see text). For the work of Morrical *et al.* we know only the total CO_2 focal area, which is given as 3.2×10^{-2} cm^2. Since we do not know the spatial profile of the laser used by Morrical and colleagues, we can consider a worst case scenario in which their laser spot has a top-hat profile with a uniform energy distribution across the whole profile. This would result in the aerosols being exposed to only 40% of the energy as in the Gaussian profile case. The data point shown in (b) does not account for any differences in laser profile; however, we have added a horizontal arrow which shows where the point from their work would fall with relation to the data from this study if this correction for a top-hat beam profile was made.

one would expect to see almost no molecular ion after 120 μs, which is indeed the case for the collected spectra.

It should also be noted that, in general, Nash *et al.* used much higher CO_2 pulse energies than were used in this study. This discrepancy might be due to the much higher mass of the particles used by Nash *et al.*, or it might be due to differences in the CO_2 beam profiles of the two lasers used. Despite some uncertainty in comparing the CO_2 pulse energies from the two experiments directly, we have attempted to scale the two sets of data to account for some of the possible discrepancies. In the study of Nash *et al.* a plateau starting at around 150 mJ per pulse was observed in the plot of total ion signal *versus* vaporization energy. This could indicate the onset of complete vaporization of the particles. In the ion trap experiments the dependence of the total ion signal on CO_2 pulse energy became less steep after an energy of approximately 25 mJ per pulse was reached, although a true leveling was never observed. In Fig. 6a we have plotted a line that shows where the values of Nash *et al.* would fall if we scaled their energies so that the leveling seen in the ion trap signal overlapped the beginning of the plateau in their data. Even with this adjustment made, the fragmentation is much more extensive in the ion trap experiments.

An interesting consequence of the different degrees of fragmentation seen for the ion trap and TOF systems is that it gives some insight into when the decomposition of oleic acid occurs. In the previous section we discussed how the observed appearance energies for oleic acid fragments support the idea that fragmentation is occurring after ionization rather than as a result of vaporization alone. The large differences between the mass spectra from this study and that of Nash *et al.* give additional evidence that fragmentation of oleic acid is occurring post-ionization. Since the time between vaporization and ionization is very similar in the two systems, one would expect to see similar ratios of parent to total ion signal if the fragmentation were occurring during this interval. The fact that much more fragmentation was seen in the ion trap system argues for a primarily post-ionization mechanism.

To further explore the differences between ion trap and TOF systems, we can compare the DHB results from the ion trap with results obtained by Morrical *et al.* using a TOF MS. Morrical *et al.* used a pulsed CO_2 laser to vaporize 1 μm DHB particles followed by REMPI using a 266 nm UV laser pulse.[11]

In this study low energy single photon ionization was used (142 nm, 8.75 eV) and decreased fragmentation compared to Morrical and co-workers was expected. This was indeed the case for low IR fluences (5×10^6 W cm^{-2}, 10 mJ per pulse) where the ratio of parent to total ion signal was close to 1, however, when the power density was raised to 1.6×10^7 W cm^{-2} (30 mJ per pulse) the ratio of parent to total ion signal dropped to only 0.15. Morrical *et al.* had a ratio of approximately 0.6 at an IR fluence of 5×10^7 W cm^{-2}.[11] Even when we introduce a correction factor to account for possible differences in CO_2 beam profile (horizontal line in Fig. 6b) the fragmentation in the ion trap experiments is considerably higher for lower IR power densities.

To obtain a better comparison with Morrical's work, we also carried out a series of experiments using resonance enhanced multiphoton ionization with a UV laser pulse at 249 nm. Even with the lowest possible CO_2 laser intensity, the ratio of parent to total ion signal in these REMPI experiments was only 0.26, considerably lower than the value of ~0.6 obtained by Morrical *et al.* Of interest is the fact that although REMPI is a soft ionization technique, it still deposits considerably more excess energy in the ions than is the case for near-threshold single photon ionization. At low vaporization energy close to 100% of the total ion signal comes from the molecular ion when SPI is used, however, when REMPI is used a maximum of 26% of the total ion signal comes from the molecular ion.

One major difference between this study and those of both Morrical *et al.* and Nash *et al.* is the size of the particles used. Morrical *et al.* used 1 μm DHB particles whereas in this work 600 nm particles were used. Nash *et al.* used 3–4 μm oleic acid particles whereas 1 μm particles were used in this work.

In order to test the effect of particle size on the degree of fragmentation, mass spectra were collected from DHB particles ranging in diameter from 300 nm to 700 nm, a factor of 12.7 change in particle volume. This change in particle size did not reveal any clear trend towards more or less fragmentation. This is not particularly surprising given that the particles are uniformly heated (see Experimental Section 2.2) and as a result the amount of IR energy absorbed per unit volume is independent of particle size.

Since particle size does not appear to be a major factor, it is likely that the higher degree of fragmentation observed for DHB in the ion trap experiments is, like the oleic acid, due to the decay of metastable ions during the long storage interval prior to mass analysis.

The conclusion that the fragmentation observed in this study is related to the type of mass spectrometer used and the long storage time in the ion trap is consistent with very recent observations by J. D. Smith and K. R. Wilson (personal communication). These researchers studied stearic acid aerosols using TOF mass analysis and observed a single peak at the molecular ion mass. When an ion trap, with storage times from 10 to 100 ms, was used in lieu of the TOF mass analyzer, only fragment ions were observed.

Metastable ion decay is a well known phenomenon in MALDI. It can be either beneficial or detrimental depending on the application. Post-source decay can be used to gain structural information from large biomolecules,[55] but it can also result in complicated mass spectra, especially for mixed samples of unknown compounds.[56] Several groups using MALDI have experimented with high pressure pulses immediately after ionization to control fragmentation by quickly thermalizing and stabilizing the metastable ions.[56–58] This high pressure pulse approach has worked well for large biomolecules in MALDI systems, and may be an option in our instrument as well.

As shown above, aerosol mass spectrometers with time-of-flight mass analyzers have an advantage over ion trap systems in that less fragmentation is observed when dealing with labile molecules. One may ask, based on this data, if a TOF mass analyzer would be more useful in an aerosol instrument. The answer to this depends on the type of molecule to be studied. The ion trap system works particularly well when using low CO_2 energies and studying more stable

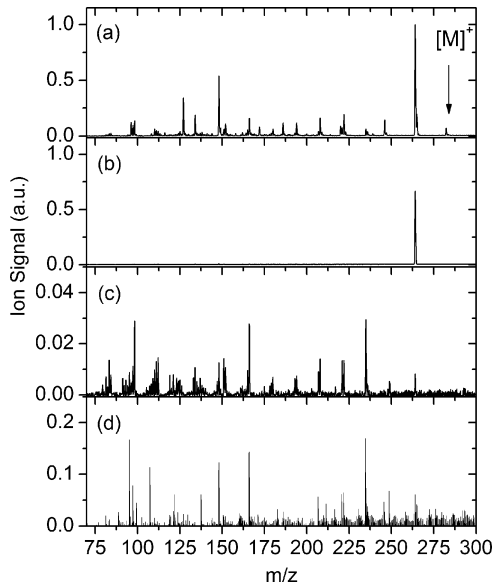

Fig. 7 Tandem MS of oleic acid, all spectra except (d) are the average of 300 laser shots. (a) Aerosol mass spectrum of oleic acid vaporized with a CO_2 energy of 7 mJ per pulse and ionized with 8.75 eV VUV photons, (b) isolation of water-loss fragment at m/z 264, (c) MS/MS spectrum of m/z 264, and (d) single particle MS/MS spectrum of m/z 264.

compounds like caffeine and DHB. In these cases only the molecular ion is observed and tandem MS can be used for positive identification. For labile molecules like oleic acid, the time-of-flight instruments have an advantage in that they give considerably less fragmentation, although even these systems do not give mass spectra consisting exclusively of molecular ion.[25,26] However, even for molecules like oleic acid, the tandem MS capabilities of the ion trap can be used to determine structural information from fragments that appear in the mass spectrum. In addition to giving structural information, MS/MS spectra from these fragments could be used as markers for specific organic molecules and for product identification. In Fig. 7 we show the MS/MS spectrum for the main fragment ion observed in the oleic acid mass spectrum. The fragmentation pattern from this ion can be used to help identify oleic acid in a mixture of compounds. The MS/MS efficiency of the ion trap is also high enough that tandem mass spectra can be collected for individual particles, although for oleic acid the signal to noise ratio for individual particles is not exceptional.

More work is needed to determine if the tandem mass spectra for individual particles will be sensitive enough for quantitative studies of complex aerosol particles. The current data suggest that the averaged MS/MS spectra will be useful for aerosol studies. (See below for an expanded discussion of possible future experiments.)

It seems reasonable to suggest that the ion trap will provide information complementary to that obtained with TOF systems, even for less stable molecules like oleic acid. Perhaps the best mass analyzer for this instrument would be a Q-TOF. This would allow both analyses of metastable ions and MS/MS experiments. Another option is to operate the ion trap at high pressures using a pulsed gas source as mentioned above. Experiments in either of these directions would be interesting.

3.5 Ion trap chemistry

In order to better understand the effect of ion storage time on the extent of fragmentation, experiments were done in which the trapping time was increased from the minimum of ~25 ms to a maximum of 830 ms. For oleic acid this increase in trapping time had no discernable effect on the extent of fragmentation, a result consistent with the decay of metastable ions on a microsecond timescale resulting in a stable distribution of ions. For DHB, however, an interesting phenomenon was observed. As the storage interval was increased to very long times, there was an increase in the fraction of ion signal at the molecular ion mass (m/z 154).

Fig. 8 shows the relative abundances of the DHB molecular ion and main fragment ion (m/z 136) as a function of trapping time and helium bath gas pressure. Extending the trapping time to several hundred milliseconds revealed an almost total conversion of the m/z 136 progeny to generate ions at m/z 154. Since ion cooling does not result in recombination of an already fragmented ion, the most plausible explanation is a reaction with background species, in this case water. In the ion trap a significant part of the background pressure comes from water vapor (based on EI mass spectra) and this water vapor could provide an ample supply for the reaction. An ion-molecule reaction of this kind is expected to be heavily

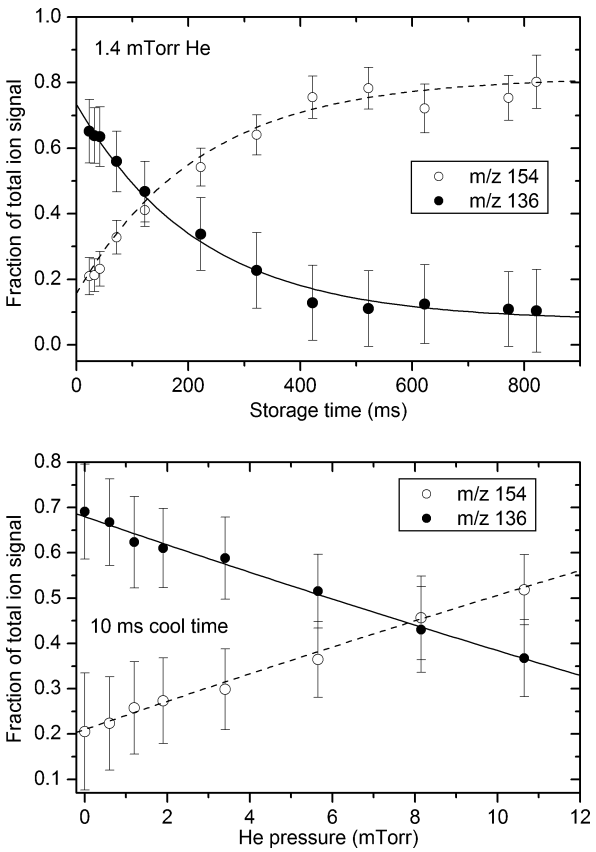

Fig. 8 Contributions of DHB ions at m/z 154 and m/z 136 to the total ion signal at 6 μs ionization delay as a function of (a) trapping time and (b) helium pressure.

pressure dependent, a fact that can be easily confirmed by varying the helium pressure (Fig. 8b). The mono-exponential dependence suggests that at the pressures used here the reaction rate is exclusively limited by the He gas pressure (Lindeman's low pressure limit). The fact that almost identical recombination yields are obtained at 34 ms cooling time with 4.4 mTorr helium and 100 ms cooling time with 1.4 mTorr helium further supports the idea of a recombination mechanism.

The observation that stored ions can undergo reactions is another effect that arises from the long storage time of ions in the trap. Reactions with a background neutral, as shown here, are a distinct possibility. Since there is no expected spatial focusing effect from longer storage times, cooling times should always be kept at a minimum (1 ms).

The fact that long storage times lead to an increased abundance of ions at the parent mass seems to suggest that we should actually see a higher fraction of molecular ions in our mass spectra when compared with the results of Morrical *et al*. since the time between ionization and mass analysis is orders of magnitude longer in our system. This would indeed be the case if the storage time in the ion trap was several hundred milliseconds rather than tens of milliseconds, however, we believe that two different processes are occurring and that the combined effect gives us low molecular ion abundances at shorter storage times. The first process is a fast decay of metastable ions that occurs on a timescale shorter than the minimum extraction time of $\sim$30 ms and leaves us with low molecular ion abundance under normal operating conditions. The second is the much slower recombination process described above that regenerates ions of m/z 154 on long timescales. Based on the extrapolated ratios from Fig. 8a, the nascent parent ratios at 0 ms storage time should be probably 25% less than those reported in Fig. 6, at 34 ms effective storage time.

3.6 Detection limits

In previous work a single particle caffeine detection limit of 8×10^5 molecules (3.5% of a pure 225 nm aerosol) with ionization at 8.75 eV (142 nm) was calculated. In the previously reported caffeine data, and the results presented here, the reported detection limits are predicated on a negligible background at the mass peak used for detection. While our pulsed technique guarantees that there will be virtually no gas background, in a complex mixed aerosol there might be an increased background from fragmentation of other components.

In addition to the caffeine data, some tentative estimates as to what the detection limits would be for other aerosol types using shorter VUV wavelengths for ionization were made in the previous study.[38] In this work we have collected DHB and oleic acid mass spectra at both 8.75 eV (142 nm) and 10.0 eV (124 nm) and we can calculate detection limits for these particles at these two VUV photon energies.

The intensity of the ion signal at a particular VUV photon energy is determined by two factors. As the VUV wavelength is shifted from 8.75 eV to 10.0 eV the number of photons per pulse is reduced by two orders of magnitude.[38] The resulting signal reduction is compensated by the increase of the molecular ionization cross-section as the VUV wavelength is shifted towards the blue away from the ionization threshold. As a result the detection limit at a particular wavelength can vary considerably from molecule to molecule.

To calculate a detection limit we average several hundred mass spectra and set a detection limit of three times the standard deviation of the baseline noise at the most intense peak. The signal to noise ratio at this most intense peak is used to determine the detection limit. Because higher vaporization energies result in more fragmentation, it is often the case that the best detection limit is achieved for a low to intermediate CO_2 laser energy where only a few peaks are very prominent.

For DHB the detection limit at 8.75 eV is $\sim 7.0 \times 10^5$ molecules. At 10.0 eV the detection limit is $\sim 1.2 \times 10^7$ molecules. These are equivalent to $\sim$2.5% and $\sim$40% of a 225 nm particle, respectively (assuming that the other compounds present do not increase the background signal level), which is relevant for our studies since the scattering detection limit in the sizing region of the aerosol mass spectrometer is $\sim$225 nm.[40] This is calculated from the measured scattering intensity of 300 nm polystyrene latex spheres which are detected with $\sim$70% efficiency. With the current optical setup the scattering detection efficiency for polystyrene latex spheres is $>$90% for particles above 400 nm.[40]

For oleic acid the detection limit at 8.75 eV is $\sim 2.6 \times 10^7$ molecules (equivalent to a pure particle diameter of $\sim$300 nm). At 10.0 eV it is $\sim 5.2 \times 10^7$ molecules (equivalent to a pure particle diameter of $\sim$375 nm). For oleic acid the minimum detectable particle sizes are larger than the scattering detection limit of the instrument, but are equivalent to $\sim$2.6% and $\sim$5.2% of a 1 μm particle, respectively.

These detection limits are more than adequate for heterogeneous studies and we anticipate that a realignment of the system to bring the CO_2, VUV, and particle beams on top of each other in the center of the ion trap will give approximately an order of magnitude increase in the ion signal (assuming instantaneous evaporation) which should substantially decrease the detection limit. If the particle is vaporized within the ionization volume, there is no need to wait for the vaporized molecules to reach the ionization region and the VUV laser can be fired at an earlier time when the vapor plume is much denser and more of the molecules are contained within the ionization zone.

Future work

This instrument is intended for use as a laboratory tool to study several processes of interest in organic aerosol chemistry. One series of measurements that will be undertaken is a study of heterogeneous reactions between PAH containing particles and oxidants such as OH, NO_3, and O_3. By studying PAH containing particles, fragmentation should be minimized. It is important to note that PAH studies can also be conducted with much simpler UV lasers and REMPI for ionization, but as shown in Fig. 6, this leads in some cases to more fragmentation than single photon ionization. In addition, unlike REMPI, the use of single photon ionization allows for the possibility of observing non-aromatic oxidation products. Also, single photon ionization is preferred for

quantitative studies since the single photon ionization cross-sections vary much less from compound to compound than REMPI cross-sections do. A tunable VUV source also allows ion appearance energies to be acquired. The value of appearance energies in identification of oxidation reaction products was demonstrated in a study of anthracene coated particles undertaken by Gloaguen *et al.*[27] With the instrument presented here both appearance energies and MS/MS can be used in compound identification providing a powerful tool for laboratory studies.

Other options for studying PAH particle chemistry include GC-MS. However, GC-MS, like our instrument, has its own set of limitation. For example, it is well known that a majority of components of organic aerosol will not be resolved in conventional GC-MS[59,60] and that even more sophisticated 2D techniques are not immune to the fact that most of the multifunctional organics cannot be eluted at all from conventional columns.[61]

In addition to heterogeneous chemistry experiments, this instrument shows some promise for characterization of real world aerosols from combustion sources which tend to contain a significant fraction of PAHs.[1,62] In these studies tunable VUV and MS/MS could again be used to help in compound identification and the single particle capabilities could be used to investigate particle-to-particle variability and extract size dependent information. More work is needed, however, to determine the usefulness of our technique for these studies. We also plan to use this instrument to study other types of heterogeneous reactions on organic particles, for example reactions between olefin containing particles and oxidants such as OH, NO_3, and O_3. We will look at these types of reactions using shorter chained olefins than oleic acid. This will reduce the energy required to vaporize the particles which may result in less fragmentation. Again, more work is needed to confirm the usefulness of the ion trap instrument for these studies.

An issue not addressed in this manuscript is quantitative detection. Preliminary work by Woods *et al.*[20] has demonstrated that single particle aerosol mass spectrometers with separate laser vaporization and ionization can give quantitative results. Preliminary work using our instrument also suggests that quantitative results may be attainable as long as the IR absorption cross-sections are not changing significantly as a function of particle composition. However, more work is required to understand the implications of particle composition and IR absorption for quantitative studies.

Conclusions

In this work DHB and oleic acid aerosols were studied using a pulsed CO_2 laser for vaporization, single photon ionization with vacuum UV, and an ion trap for mass analysis. The extent of fragmentation seen in the mass spectra was heavily dependent on both the vaporization energy and the type of molecule being studied. For DHB, a low vaporization energy gave mass spectra in which only the molecular ion was observed. In contrast, oleic acid aerosols showed quite extensive fragmentation even with low energy vaporization with the most intense peak being the water-loss fragment at m/z 264. Tandem MS was performed on this fragment and could provide a means for identifying oleic acid in mixtures.

Mass spectra from DHB and oleic acid aerosols were also collected as a function of the VUV photon energy used for ionization. Near-threshold ionization was seen to result in reduced fragmentation.

Photoionization efficiency curves were collected by continuously scanning the VUV wavelength. The appearance energies for the DHB and oleic acid molecular ions were measured and for oleic acid were found to agree well with the literature value. A literature value could not be found for DHB. The ability to determine molecular ion appearance energies together with the ability to identify organic molecules using tandem MS, should make this technique well suited for studying the reactivity of organic particles in the laboratory.[63,64]

Appearance energies for the fragment ions of DHB and oleic acid were also measured and found to be the same as those of the molecular ions within the uncertainty limits of the technique. This indicates considerable heating of the particle and offers evidence for a post-ionization fragmentation mechanism. A post-ionization fragmentation mechanism was further supported by large differences in the extent of fragmentation when comparing the ion trap results to those from aerosol mass spectrometers with time-of-flight mass analyzers.

The degree of fragmentation observed in this study, particularly for oleic acid, was considerably higher than in comparable experiments using TOF mass analyzers. This is attributed to the long storage interval in the ion trap which allows ample time for metastable ions to decay. Because of this, aerosol mass spectrometers with TOF mass analyzers have an advantage over ion trap systems in that less fragmentation is observed when dealing with labile molecules, although even TOF mass analyzers do not give exclusively molecular ion for oleic acid under similar experimental conditions.[26] It is also not possible to perform tandem MS in the time-of-flight systems currently used for aerosol mass spectrometry. Although not done in these experiments, in an ion trap it is also possible to set the trapping level so as to immediately eject low mass ions, increasing sensitivity at higher masses,[65] and resonant ejection can be used to improve mass resolution. Recent MALDI experiments suggest that the increased fragmentation observed in this study could be overcome by using high pressure pulses to quickly stabilize the metastable ions.

In addition to allowing time for the decay of metastable ions, the long storage time of the ion trap can also provide an opportunity for reactions to occur with background gases, as was seen for DHB ions held in the trap for several hundred milliseconds. The implications of long ion storage times need to be considered when carrying out aerosol studies with ion traps in order to avoid any experimental artifacts.

The detection limits for DHB and oleic acid aerosols were calculated at two VUV wavelengths. For DHB the detection limit at 8.75 eV is $\sim 7.0 \times 10^5$ molecules ($\sim 2.5\%$ of a 225 nm particle). At 10.0 eV the detection limit is $\sim 1.2 \times 10^7$ molecules ($\sim 40\%$ of a 225 nm particle). For oleic acid the

detection limit at 8.75 eV is $\sim 2.6 \times 10^7$ molecules ($\sim$2.6% of a 1 μm particle) and at 10.0 eV the detection limit is $\sim 5.2 \times 10^7$ molecules ($\sim$5.2% of a 1 μm particle). In all cases these detection limits assume that other compounds present in the particle do not raise the background signal level. These detection limits should be sufficient for studying organic reactions in the laboratory.

Acknowledgements

This work was carried out in the UBC Laboratory for Advanced Spectroscopy and Imaging Research (LASIR). Funding for this project was provided by the National Sciences and Engineering Council of Canada (NSERC), the Canadian Foundation for Climate and Atmospheric Sciences (CFCAS), the Canadian Foundation for Innovation (CFI), The British Columbia Knowledge Development Fund (BCKDF), and the NRC-NSERC-BDC Nanotechnology Initiative. The authors would also like to thank Prof. Khalid Kanan (Al Quds University) for his helpful assistance in the laboratory.

References

1 B. J. Finlayson-Pitts and J. N. Pitts, Jr., *Chemistry of the Upper and Lower Atmosphere: Theory, Experiments, and Applications*, Academic Press, New York, 2000.
2 M. Kanakidou, J. H. Seinfeld, S. N. Pandis, I. Barnes, F. J. Dentener, M. C. Facchini, R. Van Dingenen, B. Ervens, A. Nenes, C. J. Nielsen, E. Swietlicki, J. P. Putaud, Y. Balkanski, S. Fuzzi, J. Horth, G. K. Moortgat, R. Winterhalter, C. E. L. Myhre, K. Tsigaridis, E. Vignati, E. G. Stephanou and J. Wilson, *Atmos. Chem. Phys.*, 2005, **5**, 1053–1123.
3 A. R. Ravishankara and C. A. Longfellow, *Phys. Chem. Chem. Phys.*, 1999, **1**, 5433–5441.
4 Y. Rudich, *Chem. Rev.*, 2003, **103**, 5097–5124.
5 Y. Rudich, N. M. Donahue and T. F. Mentel, *Annu. Rev. Phys. Chem.*, 2007, **58**, 321–352.
6 J. J. Schauer, W. F. Rogge, L. M. Hildemann, M. A. Mazurek and G. R. Cass, *Atmos. Environ.*, 1996, **30**, 3837–3855.
7 J. J. Schauer and G. R. Cass, *Environ. Sci. Technol.*, 2000, **34**, 1821–1832.
8 C. A. Noble and K. A. Prather, *Mass Spectrom. Rev.*, 2000, **19**, 248–274.
9 D. G. Nash, T. Baer and M. V. Johnston, *Int. J. Mass Spectrom.*, 2006, **258**, 2–12.
10 D. M. Murphy, *Mass Spectrom. Rev.*, 2007, **26**, 150–165.
11 B. D. Morrical, D. P. Fergenson and K. A. Prather, *J. Am. Soc. Mass Spectrom.*, 1998, **9**, 1068–1073.
12 B. W. LaFranchi, J. Zahardis and G. A. Petrucci, *Rapid Commun. Mass Spectrom.*, 2004, **18**, 2517–2521.
13 J. D. Hearn and G. D. Smith, *Anal. Chem.*, 2004, **76**, 2820–2826.
14 W. A. Harris, P. T. A. Reilly and W. B. Whitten, *Anal. Chem.*, 2007, **79**, 2354–2358.
15 M. R. Canagaratna, J. T. Jayne, J. L. Jimenez, J. D. Allan, M. R. Alfarra, Q. Zhang, T. B. Onasch, F. Drewnick, H. Coe, A. Middlebrook, A. Delia, L. R. Williams, A. M. Trimborn, M. J. Northway, P. F. DeCarlo, C. E. Kolb, P. Davidovits and D. R. Worsnop, *Mass Spectrom. Rev.*, 2007, **26**, 185–222.
16 A. Zelenyuk, J. Cabalo, T. Baer and R. E. Miller, *Anal. Chem.*, 1999, **71**, 1802–1808.
17 A. Zelenyuk and D. Imre, *Aerosol Sci. Technol.*, 2005, **39**, 554–568.
18 A. Lazar, P. T. A. Reilly, W. B. Whitten and J. M. Ramsey, *Environ. Sci. Technol.*, 1999, **33**, 3993–4001.
19 M. Bente, T. Adam, T. Ferge, S. Gallavardin, M. Sklorz, T. Streibel and R. Zimmermann, *Int. J. Mass Spectrom.*, 2006, **258**, 86–94.
20 E. Woods, G. D. Smith, Y. Dessiaterik, T. Baer and R. E. Miller, *Anal. Chem.*, 2001, **73**, 2317–2322.
21 B. Oktem, M. P. Tolocka and M. V. Johnston, *Anal. Chem.*, 2004, **76**, 253–261.
22 T. Ferge, F. Muhlberger and R. Zimmermann, *Anal. Chem.*, 2005, **77**, 4528–4538.
23 J. N. Shu, S. K. Gao and Y. Li, *Aerosol Sci. Technol.*, 2008, **42**, 110–113.
24 M. J. Northway, J. T. Jayne, D. W. Toohey, M. R. Canagaratna, A. Trimborn, K. I. Akiyama, A. Shimono, J. L. Jimenez, P. F. DeCarlo, K. R. Wilson and D. R. Worsnop, *Aerosol Sci. Technol.*, 2007, **41**, 828–839.
25 E. R. Mysak, K. R. Wilson, M. Jimenez-Cruz, M. Ahmed and T. Baer, *Anal. Chem.*, 2005, **77**, 5953–5960.
26 D. G. Nash, X. F. Liu, E. R. Mysak and T. Baer, *Int. J. Mass Spectrom.*, 2005, **241**, 89–97.
27 E. Gloaguen, E. R. Mysak, S. R. Leone, M. Ahmed and K. R. Wilson, *Int. J. Mass Spectrom.*, 2006, **258**, 74–85.
28 D. C. Sykes, E. Woods, G. D. Smith, T. Baer and R. E. Miller, *Anal. Chem.*, 2002, **74**, 2048–2052.
29 E. Woods, G. D. Smith, R. E. Miller and T. Baer, *Anal. Chem.*, 2002, **74**, 1642–1649.
30 J. M. Dale, M. Yang, W. B. Whitten and J. M. Ramsey, *Anal. Chem.*, 1994, **66**, 3431–3435.
31 M. Yang, J. M. Dale, W. B. Whitten and J. M. Ramsey, *Anal. Chem.*, 1995, **67**, 1021–1025.
32 M. Yang, P. T. A. Reilly, K. B. Boraas, W. B. Whitten and J. M. Ramsey, *Rapid Commun. Mass Spectrom.*, 1996, **10**, 347–351.
33 P. T. A. Reilly, R. A. Gieray, M. Yang, W. B. Whitten and J. M. Ramsey, *Anal. Chem.*, 1997, **69**, 36–39.
34 A. C. Lazar, P. T. A. Reilly, W. B. Whitten and J. M. Ramsey, *Anal. Chem.*, 2000, **72**, 2142–2147.
35 A. Kurten, J. Curtius, F. Helleis, E. R. Lovejoy and S. Borrmann, *Int. J. Mass Spectrom.*, 2007, **265**, 30–39.
36 W. A. Harris, P. T. A. Reilly and W. B. Whitten, *Anal. Chem.*, 2005, **77**, 4042–4050.
37 W. A. Harris, P. T. A. Reilly and W. B. Whitten, *Int. J. Mass Spectrom.*, 2006, **258**, 113–119.
38 S. J. Hanna, P. Campuzano-Jost, E. A. Simpson, D. B. Robb, I. Burak, M. W. Blades, J. H. Hepburn and A. K. Bertram, *Int. J. Mass Spectrom.*, 2009, **279**, 134–146.
39 *NIST Chemistry WebBook*, ed. P. J. Linstrom and W. G. Mallard, National Institute of Standards and Technology, Gaithersburg, MD, 20899, 2005.
40 E. A. Simpson, P. Campuzano-Jost, S. J. Hanna, D. B. Robb, J. H. Hepburn, M. W. Blades and A. K. Bertram, *Int. J. Mass Spectrom.*, 2009, **281**, 140–149.
41 P. Liu, P. J. Ziemann, D. B. Kittelson and P. H. McMurry, *Aerosol Sci. Technol.*, 1995, **22**, 314–324.
42 P. Liu, P. J. Ziemann, D. B. Kittelson and P. H. McMurry, *Aerosol Sci. Technol.*, 1995, **22**, 293–313.
43 E. Woods, R. E. Miller and T. Baer, *J. Phys. Chem. A*, 2003, **107**, 2119–2125.
44 G. C. Stafford, P. E. Kelley, J. E. P. Syka, W. E. Reynolds and J. F. J. Todd, *Int. J. Mass Spectrom. Ion Processes*, 1984, **60**, 85–98.
45 V. M. Doroshenko and R. J. Cotter, *Rapid Commun. Mass Spectrom.*, 1996, **10**, 65–73.
46 D. E. Goeringer and S. A. McLuckey, *J. Chem. Phys.*, 1996, **104**, 2214–2221.
47 M. H. Soni and R. G. Cooks, *Anal. Chem.*, 1994, **66**, 2488–2496.
48 R. K. Julian and R. G. Cooks, *Anal. Chem.*, 1993, **65**, 1827–1833.
49 S. Kinugasa, K. Tanabe and T. Tamura, *Spectral Database of Organic Compounds*, National Institute of Advanced Industrial Science and Technology (AIST), Japan.
50 Y. J. Shi and R. H. Lipson, *Can. J. Chem.*, 2005, **83**, 1891–1902.
51 S. E. Vanbramer and M. V. Johnston, *J. Am. Soc. Mass Spectrom.*, 1990, **1**, 419–426.
52 K. R. Wilson, M. Jimenez-Cruz, C. Nicolas, L. Belau, S. R. Leone and M. Ahmed, *J. Phys. Chem. A*, 2006, **110**, 2106–2113.
53 W. Genuit and N. M. M. Nibbering, *Int. J. Mass Spectrom. Ion Processes*, 1986, **73**, 61–80.
54 B. Steiner, C. F. Giese and M. G. Inghram, *J. Chem. Phys.*, 1961, **34**, 189–220.
55 B. Spengler, *J. Mass Spectrom.*, 1997, **32**, 1019–1036.

56 P. B. O'Connor and C. E. Costello, *Rapid Commun. Mass Spectrom.*, 2001, **15**, 1862–1868.
57 V. V. Laiko, M. A. Baldwin and A. L. Burlingame, *Anal. Chem.*, 2000, **72**, 652–657.
58 D. Papanastasiou, O. Belgacem, M. Sudakov and E. Raptakis, *Rev. Sci. Instrum.*, 2008, **79**, 055103.
59 W. F. Rogge, M. A. Mazurek, L. M. Hildemann, G. R. Cass and B. R. T. Simoneit, *Atmos. Environ., Part A*, 1993, **27**, 1309–1330.
60 B. J. Williams, A. H. Goldstein, D. B. Millet, R. Holzinger, N. M. Kreisberg, S. V. Hering, A. B. White, D. R. Worsnop, J. D. Allan and J. L. Jimenez, *J. Geophys. Res., [Atmos.]*, 2007, **112**, D10S26.
61 A. H. Goldstein, D. R. Worton, B. J. Williams, S. V. Hering, N. M. Kreisberg, O. Panic and T. Gorecki, *J. Chromatogr., A*, 2008, **1186**, 340–347.
62 K. P. Hinz and B. Spengler, *J. Mass Spectrom.*, 2007, **42**, 843–860.
63 S. Gross and A. K. Bertram, *J. Phys. Chem. A*, 2008, **112**, 3104–3113.
64 J. Mak, S. Gross and A. K. Bertram, *Geophys. Res. Lett.*, 2007, **34**, L10804.
65 W. A. Harris, P. T. A. Reilly, W. B. Whitten and J. M. Ramsey, *Rev. Sci. Instrum.*, 2005, **76**, 064102.
66 J. Cabalo, A. Zelenyuk, T. Baer and R. E. Miller, *Aerosol Sci. Technol.*, 2000, **33**, 3–19.